Journal of Hydrology 631 (2024) 130671

Contents lists available at ScienceDirect

Journal of Hydrology

journal homepage: www.elsevier.com/locate/jhydrol

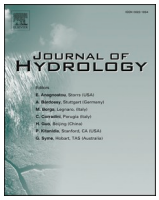

Research papers

Importance of forest stand structures for gross rainfall partitioning on China's Loess Plateau

Xu Hu [a,b], Zhaoqi Fu [a,b], Ge Sun [c], Biao Wang [a,b], Keyan Liu [a,b], Churui Zhang [a,b], Lu Han [a,b], Lixin Chen [a,b,*], Zhiqiang Zhang [a,b,*]

[a] College of Soil and Water Conservation, Beijing Forestry University, Beijing 100083, China
[b] Forest Ecosystem Studies, National Observation and Research Station, Ji Country, Shanxi 042200, China
[c] Eastern Forest Environmental Threat Assessment Center, Southern Research Station, USDA Forest Service, Research Triangle Park, NC 27709, USA

ARTICLE INFO

This manuscript was handled by Marco Borga, Editor-in-Chief, with the assistance of Yasuto Tachikawa, Associate Editor

Keywords:
Rainfall redistribution
Species comparison
Structural traits
Boosted regression trees

ABSTRACT

Large-scale ecological restoration in the arid and semi-arid Loess Plateau region of northern China is challenged by the intensifying water stress due to the changes in precipitation regimes. Although the importance of Gross Precipitation Partitioning (GRP) has been well recognized in forest hydrology, especially in dry areas, the processes are not understood because site- or region-specific factors complicate the accurate quantifications. This study integrates meta-analysis and field observation to compare patterns of GRP in forest stands that had different origins (plantations vs. native forests) and tree species (deciduous vs. evergreen) compositions. We aimed at quantifying the dominant biotic and abiotic factors controlling each of the GRP components to form empirical relationships between the GRP components and the influencing factors via the Boosted Regression Trees (BRT) model. We found a convergence in the GRP components among the examined stands that have diverse tree species and origins. Our results indicated that, unlike stem flow (SF) and canopy interception (I_c), the throughfall (TF) did not differ between natural and plantation stands. Meanwhile, from the perspective of species composition, the broadleaf forest stands had significantly higher SF rates than the coniferous stands. We found that stand structures exerted limited influence on TF, but significantly affected SF and I_c. We hypothesized that the residence time of the GRP components was important in explaining the matrix of influencing factors. The cumulative influences of stand structure factors played a more important role than species in most conditions. Based on the most influential factors (cumulative explanatory power > 70 %) selected from the BRT model, we successfully built a general formula to represent the GRP processes across the diverse forest stands in the Loess Plateau. Our study provides insights into the underlying mechanism of GRP for developing more realistic forest hydrological models. An improved understanding of GRP and better models are important for guiding large scale reforestation efforts that account for hydrological processes across stand species and origins.

1. Introduction

Afforestation has been adopted as a major ecological restoration effort in arid/semiarid areas, raising wide concerns regarding their hydrological impact on water resources (Sun et al., 2006; Adane and Gates, 2015; Lima et al., 2012; Wang et al., 2011). Besides the substantial water consumption by tree transpiration, critics also center around the reduction of throughfall (TF) through the process of canopy interception (I_c) (Magliano et al., 2019). For arid and semi-arid areas, I_c accounts for up to 17 %–44 % of the total precipitation across stands of different densities and species composition, leading to a variation of TF of 47 %–84 % (Sun et al., 2018; Ding et al., 2021; Ma et al., 2019; Skhosana et al., 2023; Yang et al., 2023). From this perspective, the canopy rainfall partitioning directly influences the amount of available soil water to sustain vegetation functioning, which is crucial in water-limited regions/periods. Therefore, accurately characterizing the gross rainfall partitioning (GRP) processes is important for quantifying water availability and rainfall-to-runoff hydrological processes under a changing climate (Lian et al., 2022).

Many abiotic and biotic factors control GRP (An et al., 2022; de Lima and Tonello, 2023; Rodrigues et al., 2019; Yue et al., 2021; Zhu et al., 2021). Site-level variances of GRP have been mainly ascribed to (1)

* Corresponding authors at: College of Soil and Water Conservation, Beijing Forestry University, Beijing 100083, China.
E-mail addresses: ge.sun@usda.gov (G. Sun), myclover17@bjfu.edu.cn (L. Chen), zhqzhang@bjfu.edu.cn (Z. Zhang).

https://doi.org/10.1016/j.jhydrol.2024.130671
Received 5 August 2023; Received in revised form 8 November 2023; Accepted 30 December 2023
Available online 24 January 2024

hydro-meteorological factors (e.g. vapor pressure deficit (VPD), rainfall characteristics, and temperature *etc*.) (Siegert and Levia, 2014; Tanaka et al., 2017; Zhang et al., 2015) which directly influence the canopy interception loading and the evaporation rate of the canopy interception, and (2) stand attributes, such as crown structure (Brauman et al., 2010; Pflug et al., 2021; Zhang et al., 2017), height (Sadeghi et al., 2020; Li et al., 2016; Yue et al., 2021), stem density and DBH (Shinohara et al., 2015), and species composition (Cano-Arboleda et al., 2022; Zhang et al., 2022). Existing studies have only examined limited aspects of variables (Honda et al., 2015; Zabret and Sraj, 2019; Zhang et al., 2017) or several related variables (Zabret et al., 2018; Zong et al., 2021) in a separate manner. Therefore, the relationship between stand attributes and canopy rainfall redistribution remains poorly understood. For example, stand structural traits and species identity are usually intertwined in the determination of stand GRP (Zhang et al., 2022). However, many studies attributed the influences of species identity to their contrasting structural traits (Zhang et al., 2022).

The determinants of GRP fluxes vary with scale. On an individual tree scale, the GRP differences are caused by the tree morphological structures based on plant taxonomy. However, at forest stand or even larger scales, the structural characteristics of different tree species are combined to form collective stand characteristics. Therefore, given that the GRP rarely involves any physiological process, it is reasonable to hypothesize that stand structural characteristics would be more important than tree species identity in influencing the GRP as the scale increases. This hypothesis might also explain the inconsistent forest stand water balance-species relationship. Trees grow and thus lead to changes in forest stand structure, resulting in temporal variability of water balance relationships in the same area (Dong et al., 2020; Forrester, 2019). However, the large variability of background environmental factors may hinder testing this hypothesis. For example, precipitation characteristics can further increase within-species or between-species variability (Zhang et al., 2021), making it difficult to separate the effects of forest stand characteristics from species on water cycles. Synchronized on-site observations create a consistent environmental condition, and thus eliminate the interferences from cross-stand structure factors.

It is reasonable to hypothesize that stand structural attributes triumph over the tree species identity or diversity in influencing the rainfall partitioning processes because (1) rainfall partitioning is more a physical process than a physiological process and (2) the evaluation of stand level GRP partitioning was influenced by the average structure rather than the individuals. Predictive models based on accessible stand structure variables would facilitate the assessment of forest water cycles for managed forests (Sun et al., 2023). However, only a limited number of studies have simultaneously analyzed the full range of influencing factors. Such studies are greatly needed to a holistic understanding GRP mechanism and lay the foundation for accurate estimation of local canopy and stand water balances. Such knowledge would also better elucidate the contrasting hydrological responses of different forest types for landscape ecological restoration.

The overarching objective of this study is to unravel the shared dynamics and quantitative relationship between stand traits and GRP partitioning process across different stand types. Specially, we aim to: (i) investigate the GRP partitioning for these common forest types in the semi-arid region, (ii) identify stand characteristics that dominate GRP partitioning and develop empirical relationships by Boosted Regression Trees (BRT) method, and (iii) test the general applicability of the structural-GRP relationship across the region.

2. Method and materials

2.1. Site description of the field observation

We integrated on-site field observation (Section 2.1-2.4) and data mining (Section 2.5) to better represent the spatial and temporal heterogeneity of GRP in the Loess Plateau. We performed our study in Caijiachuan watershed (36°14′–36°18′ N, 110°39′–110°47′ E, 900–1513 m elevation), Shanxi province, China. The watershed has been a part of large-scale of eco-restoration campaign across the Loess Plateau since 1990s. The site is mainly covered by plantations and in some areas the orchards. The site has a warm temperate continental monsoon climate. The annual temperature was averaged at 10 °C and the annual precipitation was concentrated from July to September (based on average 1956–2021 climate data) at an average value of 580 mm (Feng et al., 2023). Challenged by severe soil erosion and decreased ecosystem services in the Loess Plateau of China (Gao et al., 2016; Yu et al., 2015; Zhao et al., 2013), the afforestation campaign has been carried out since the 1950s (Jia et al., 2017). This area witnesses a 25 % increase of vegetation coverage over the last decade (Feng et al., 2016).

2.2. Survey of the plots

We selected 20 plots (Fig. 1, Table 1) to represent all tree species adopted in the local eco-restoration project. Therefore, the monoculture and mixing stands were considered to enable the comparison among species and morphological structures.

The comprehensive plot survey (Table 1) was conducted in May 2022. Diameter at breast height (DBH) of different individual was measured with a tape measure. The tree height (TH) was measured by visual method. TH measurement of all trees were conducted by one person to reduce the artificial bias. By assuming the canopy took the shape of an ellipse, the canopy area (CA) could be calculated using the formula of the area of an ellipse: $CA = \Pi \times d_1 \times d_2/4$, where d_1 and d_2 are east–west and north–south directions diameters through the center of canopy, respectively (Su et al., 2016). LAI was observed with SunScan canopy analyzer (Delta-T Devices Cambridge, UK) every month to track canopy structure changes throughout the growing season.

2.3. Measurements of the rainfall partitioning components

All components of rainfall partitioning process were observed and recorded from Jun to Sep 2022 with both totalizing and tipping-bucket rain gauges. The tipping gauge stored the rainfall event process every 15 min at the resolution of 0.254 mm (WatchDog 1120 Rain Gauge) and stored it in a time-step. The stored data were downloaded using SpecWare 9 Pro software (Spectrum Technologies, Inc., Aurora, IL). Totalizing gauge were also used to back up the insufficiency of tipping bucket rain gauges. The rain was drained into a 25 L barrel and the readings were obtained with a measuring cup ranging from 0.1 L to 2.0 L.

2.3.1. Event selection

The rainfall events were defined by a break in rainfall of at least 12 h. This rainless interval allows the evaporation of previously intercepted water and thus the following event would be reset with zero canopy interception (Blume et al., 2022; Spencer and Meerveld, 2016). Events with measured TF higher than GR by $\geq$1 mm because of either spatial-heterogeneity of canopy input or technical failures were excluded from the analysis.

2.3.2. Measurements of GRP components

For measuring gross rainfall, tipping bucket gauges were mounted atop the 30 m eddy covariance tower within an average 1 km of our sampling plots. We also had a tipping bucket installed in the station courtyard at the foot of the examined mountainous watershed. The readings of the two measurements location presented good agreement ($R^2 = 0.90$).

2.3.2.1. Throughfall (TF). We made 0.3 (width) × 1 (long) × 0.15 m (height) metal troughs for TF measurements. Each trough was connected with a totalizing gauge. We installed two of such trough units at each plot in a transactional fashion to improve the spatial representativeness

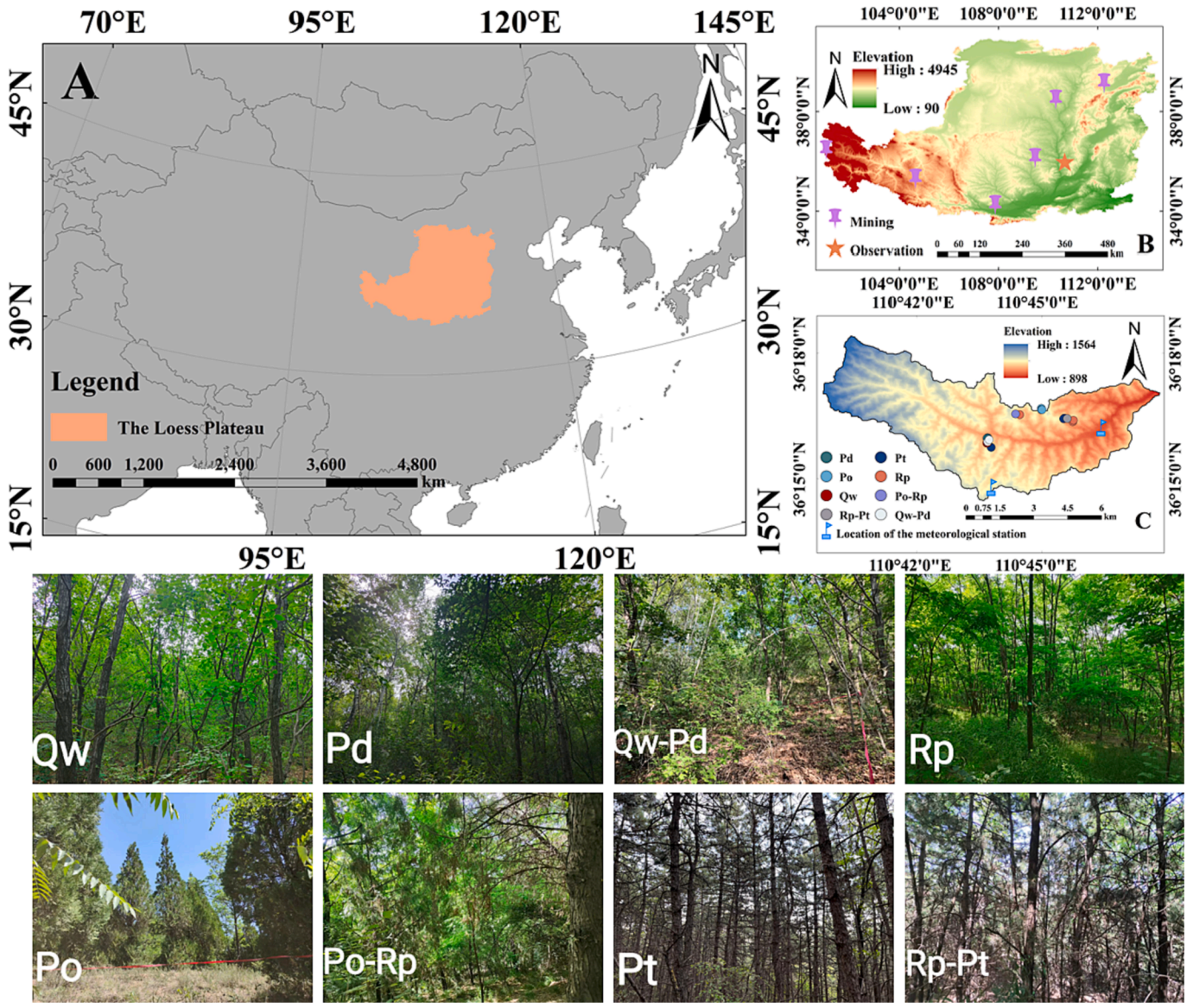

Fig. 1. The study site locations and stand characteristics. A: the extent of the Loess Plateau; B: the location of the study watershed on the Loess Plateau, therein the orange pentacle is the research site- Caijiachuan watershed, and the purple thumbtack is the location of data mining; C: the locations of the experimental plots in the Caijiachuan watershed. Different colored dots represent different stands as illustrated in the lower left corner. The field photos of all stands are below the A and C. Qw: Pure forest of *Q. wutaishanica*; Pd: Pure forest of *P. davidiana*; Qw-Pd: Mixed forest of Q. *wutaishanica* and *P. davidiana*; Rp: Pure forest of *R. pseudoacacia*; Po: Pure forest of *P. orientalis*; Po-Rp: Mixed forest of *P. orientalis* and *R. pseudoacacia*; Pt: Pure forest of *P. tabuliformis*; Rp-Pt: Mixed forest of *R. pseudoacacia* and *P. tabuliformis*. Abbreviations are used throughout this article. (For interpretation of the references to colour in this figure legend, the reader is referred to the web version of this article.)

of through fall and thus saved the number of the tipping buckets. The trough units were elevated 20 cm above the ground on the wooden stakes to avoid mud splashing or obstruction by other masses from the ground. The meshes covered the gauges to prevent fallen leaves and debris from clogging the drainage pipe. The intercepted debris atop the meshes were cleaned every 3–4 days during the growing season. Throughfall was collected after each rain event. We took a few measures to reduce the evaporation loss from the troughs to a negligible rate. They included: (1) coating the inner side of the troughs with hydrophobic paint, (2) setting the troughs in a slightly titled way. Additionally, we regularly clean the troughs to avoid litter and dust diminishing or absorbing the water flow, (3) using air-tight barrels to collect the water, and (4) retrieving the readings as soon as the rainfall events stopped.

2.3.2.2. Stem flow (SF). SF was measured individually on site-basis. DBH can be divided into three classes according to cluster analysis. We selected 2 trees per DBH class in each site. The enveloping water collection method was used to collect stemflow. We wrapped the tree trunk with impermeable material, then stick the hose pipe to the impermeable material with nails. Silicone sealant was filled in the fissures between the pipe and the bark. The pipe drained the SF into a 25 L barrel. The stemflow containers were cleaned at least once a week to prevent clogging and spillage. Some containers overflowed during the events of heavy rainfall and thus were excluded from further analysis. SF is calculated according to Eq. (1):

$$SF = \sum_{i=1}^{n} \frac{C_i \times M_i}{S \times 10^3} \quad (1)$$

where SF is the stemflow (mm), C_i is the i_{th}-diameter stemflow (ml), n is the number of tree trunks, M_i is the number of trees at diameter i, and S is the area of the plot (m^2).

Table 1
Descriptive statistics of the stands.

Stand	DBH (cm)	Tree height (m)	Canopy area (m^2)	Stand Density (trees·ha^{-1})	LAI (m^2/m^2)	Origin	Leaf type	Plot number from our field study	References
Qw	11.5 ± 3.4	8.9 ± 1.9	9.2 ± 10.2	1193 ± 256	5.8	Natural	Broadleaf	2	Wang et al., 2022; Cheng, 2020
Qw-Pd	10.9 ± 3.6	9.2 ± 2.4	6.9 ± 4.6	1575 ± 200	5.3	Natural	Broadleaf	2	——
Pd	11.1 ± 3.1	7.7 ± 0.7	5.6 ± 4.5	1162 ± 12	5.6	Natural	Broadleaf	2	——
Rp	13.5 ± 5.3	12.0 ± 2.7	12.7 ± 9.2	1992 ± 800	4.9	Plantation	Broadleaf	3	Li et al., 2022; Wang et al., 2022; Cheng, 2020; Gao, 2019
Po-Rp	12.2 ± 4.2	9.0 ± 2.7	15.2 ± 8.8	1225 ± 425	5.5	Plantation	Mixed	2	——
Pt	13.7 ± 3.3	7.5 ± 1.6	13.9 ± 9.1	1224 ± 578	4.1	Plantation	Coniferous	3	Li et al., 2022; Ma et al., 2022; Gao, 2019; Yang et al., 2019; Jian et al., 2015; Zhang, 2020; Dong et al., 2020
Rp-Pt	11.5 ± 3.9	8.6 ± 1.8	15.8 ± 10.6	2067 ± 155	5.9	Plantation	Mixed	3	——
Po	10.6 ± 3.3	6.2 ± 1.6	7.8 ± 4.7	1256 ± 282	3.9	Plantation	Coniferous	3	Gao, 2019
Bp	17.4 ± 9.2	11.3 ± 4.8	7.3 ± 6.0	3191 ± 944	3.1	Plantation	Broadleaf	0	Huang et al., 2018

Note: Data sources include our field observations and data mining. Field observations cover all types of the stand and references involving the same tree species as our field observation are listed at the end.
All the plots involved in our field observations are 400 m^2.

Table 2
Abbreviations and units for factors used in the BRT analysis.

Factors	Variables	Abbreviation	Unit
Biotic	Diameter at breast height	DBH	cm
	Tree height	TH	m
	Canopy area	CA	m^2
	Forest type	Species	NA
	Stand density	TD	trees·ha^{-1}
	Leaf area index	LAI	m^2/m^2
	Phenology(deciduous, evergreen, mixed)	Phenology	NA
	Leaf type	Leaf	NA
Environmental	Precipitation	P	mm
	Average rainfall intensity	I	mm/h
	Maximum rainfall intensity in 30 min	I30	mm/h
	Rainfall duration	D	h
	Number of non-rainy days before the rainfall event	ADP	day
	Rainless interval within a single event	IEI	h
	Ambient temperature	T	℃
	Net radiation	Rn	W/m^2
	Wind speed	WS	m/s
	Relative humidity	RH	%
	Vapor pressure deficit	VPD	KPa

2.3.2.3. Canopy interception (I_c). I_c was derived based on the principle of water balance as Eq. (2) since it cannot be observed directly:

$$I_c = P - N = P - (TF + SF) \quad (2)$$

where I_c stands for the interception (mm), P for the GR depth (mm), N for the net rainfall depth (mm), TF for the throughfall depth (mm), and SF is the stemflow depth (mm).

2.4. Environmental factors

Meteorological variables, including solar radiation, relative humidity, temperature, and gross rainfall, were automatically recorded by the monitor stations (AWS, Campbell, Logan, USA) and the eddy covariance flux tower nearby within the same watershed.

2.5. Data mining

To improve the spatial and temporal representativeness, we surveyed related studies on the Web of Science and China National Knowledge Infrastructure (CNKI) to retrieve published GRP data in the loess area from 2015 to 2021. We employed the keyword "throughfall", "stemflow", "interception", "rainfall partitioning", "precipitation partitioning", and "rainfall redistribution" (Zhang et al., 2023c). We screened the retrieved paper for further analysis based on the following criteria: (a) studies was conducted only on the Loess Plateau; (b) the study provided field data instead of modeled data on secondary rainfall scale; (c) average tree height, average DBH, average crown area and stand density, as well as rainfall amount and rainfall duration were described or could be derived. We retrieved 10 papers (Appendix S1) and extracted data by the GetData software (2.22) from the tables in the text or from the figures. We finally got 339 valid samples in total, including 121 for throughfall, 60 for stemflow, and 158 for canopy interception, and the structural data of the corresponding stand (Fig. 2). The literature data were mingled with our own observation to form a data pool for further Boosted Regression Trees (BRT) analysis.

2.6. Boosted Regression Trees (BRT) for the identification of the influencing factors

BRT has been widely used in recent studies on I_c (Yu et al., 2022; Zabret and Sraj, 2021; Zhang et al., 2023c). Boosted model combines multiple simple models to enhance the predictive performance. This approach integrates the advantages of regression trees with that of the boosted model, and thus improve the accuracy and reduces overfitting by introducing randomness into a boosted model (Elith et al., 2008).

We adopted BRT to evaluate the influences of individual stand structural and environmental factors on TF, SF, and I_c. The predicting variables included (1) rainfall characteristic, namely the amount, intensity, maximum rainfall intensity in 30 min, event duration, number of non-rainy days before the rainfall event and rainless interval within a single event, (2) meteorological variables, including ambient temperature, net radiation, relative humidity (RH), wind speed (WS) and vapor pressure deficit (VPD), (3) stand structural features, i.e., diameter at breast height (DBH), tree height (TH), canopy area, stand density, and leaf area index (LAI), (4) biotic factors, i.e., forest type, phenology

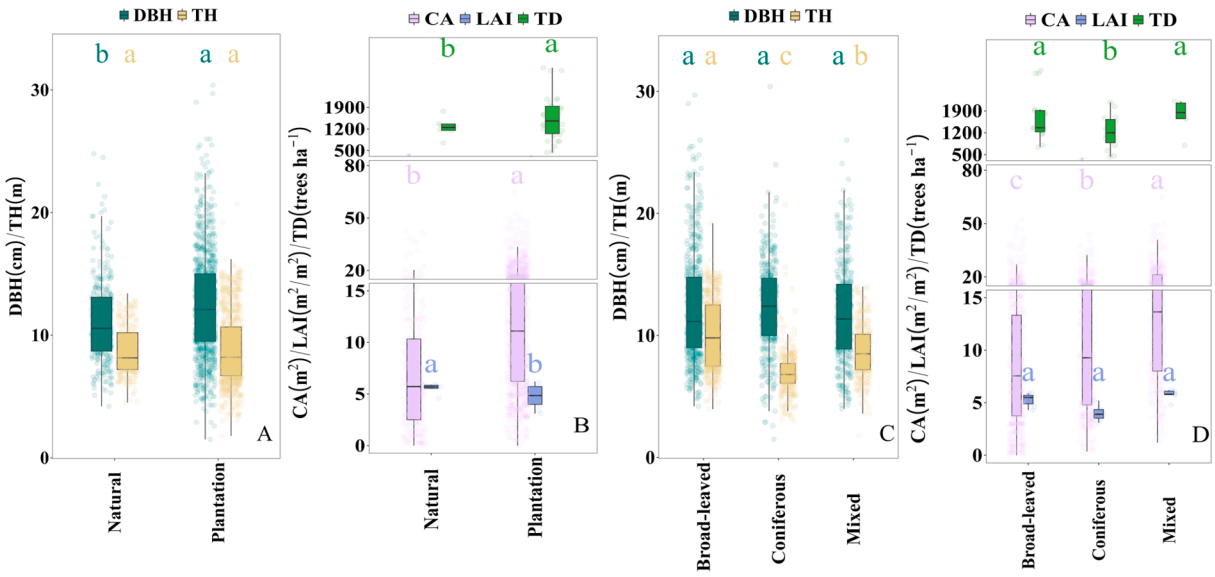

Fig. 2. Basic information of vegetation of study sites. Stand basic information includes DBH, TH, CA, TD and LAI. (A) and (B) represent Natural and Plantation forest; (C) and (D) represent Broad-leaved, Coniferous and Mixed forest. Abbreviations in the figure can be found in Table 2. Significant differences of indicators between different types of stands were represented by different lowercase letters in corresponding colors (One-way ANOVA, $P < 0.05$). On-site observations and extracted data from data mining are represented.

(deciduous, evergreen and mixed) and leaf type.

We used 75 % of the data pool to establish our predictive BRT model and the rest 25 % of the data served as the test dataset which was used to test the performance of the BRT model. We fitted BRT using the Gaussian response. We set the learning rate, the tree complexity and the bag fraction at 0.005, 5 and 0.5, respectively. A model with at least 1000 trees was regarded qualified based on a rule of thumb (Elith et al., 2008). Relative influence value (RI) of predictor variable on the response variable was calculated as a function of the number of times the variable was split. A weighted average of RIs was evaluated by dividing the squared improvement to model by the number of splits (Elith et al., 2008). Each variable's RI was scaled to 100. Response variables were influenced more strongly by higher values. We used partial dependence plots (PDP) to demonstrate the impact of individual predictor on RI for the factors with cumulative explanatory power over 70 %. The means of 500 bootstrap replicates were estimated with 95 % confidence intervals. We run BRT models with the package "gbm" (Ridgeway, 2015) in R studio.

2.7. Statistical analysis

The threshold rainfall for throughfall and stemflow initiation was determined by regression equations between individual precipitation depth and individual throughfall or stemflow, respectively (Yuan et al., 2016; Zhang et al., 2015). One-way ANOVA was used to test the significant differences of the percentages of TF, SF, and I_c under different stands and the significant differences of the threshold values of the TF and SF. The quantity regression analysis was conducted between different GRP components and rainfall characteristics (rainfall amount, rainfall intensity and rainfall duration). Hierarchical multiple regression analysis was used to evaluate the key indicators affecting the rainfall redistribution process. Relationships among structural variables was represented by correlation matrix plot in R "PerformanceAnalytics" package (Peterson and Carl, 2019). The performances of the BRT model and other research model were compared using the slope, the RMSE, and Nash–Sutcliffe model efficiency (NSE). All statistical analysis and plotting were conducted in R version 4.2.2 (R core team, 2022). Statistical significance was confirmed with $p < 0.05$ for all analyses.

3. Results

3.1. Hydrological dynamics of the rainfall redistribution processes

The event-based gross precipitation ranged from 4.2 to 140.4 mm (Fig. 3A) with an average duration of 16.6 ± 22.8 h and average intensity of 7.6 ± 15.3 mm/h.

On an event base, the site-specific TF varied from 2.4 mm to 56.1 mm, accounting for 24.5–95.7 % of the corresponding incident rainfall (Fig. 3B, Fig. S1). SF contributed below 13.6 % of net precipitation (Fig. 3C, Fig. S1). Interception contributed 0.7 % to 86.2 % of gross precipitation (Fig. 3D, Fig. S1). The pure stand and the mixed stand that shared same species demonstrated similar ratios of TF, SF and I_c ($p > 0.05$), such as in the stand-pairs of Pt-RpPt (Fig. 3).

Consistent across all stands, TF was significantly influenced by stemflow and canopy interception (Fig. 4 B and C). The increase of canopy interception significantly reduced the ratio of throughfall ($R^2 = 0.87$) and stemflow ($R^2 = 0.32$). TF varied in consistency with the stemflow ($R^2 = 0.13$), but the TF ratio stayed at a relatively saturated status as the stem flow increased.

3.2. Variations of rainfall redistribution components across different stands

From the perspective of stand origin, the natural forests demonstrated significantly higher I_c and lower SF than plantations. No significant differences were observed in TF between these two types of stands (Table 3). Meanwhile, the GRP components demonstrated no significant differences when compared among groups of varied species compositions (Table 3).

Significant differences were found between the thresholds of TF and SF initiation on an event basis (Table 4). Plantations demonstrated significantly higher initiation threshold of TF in comparison with natural forests ($p < 0.05$). The coniferous stands showed significantly higher TF than the broadleaf stands ($p < 0.05$) but not than the mixed stands ($p > 0.05$). Meanwhile, no significant differences of SF initiation values were found among different types of stands ($p > 0.05$).

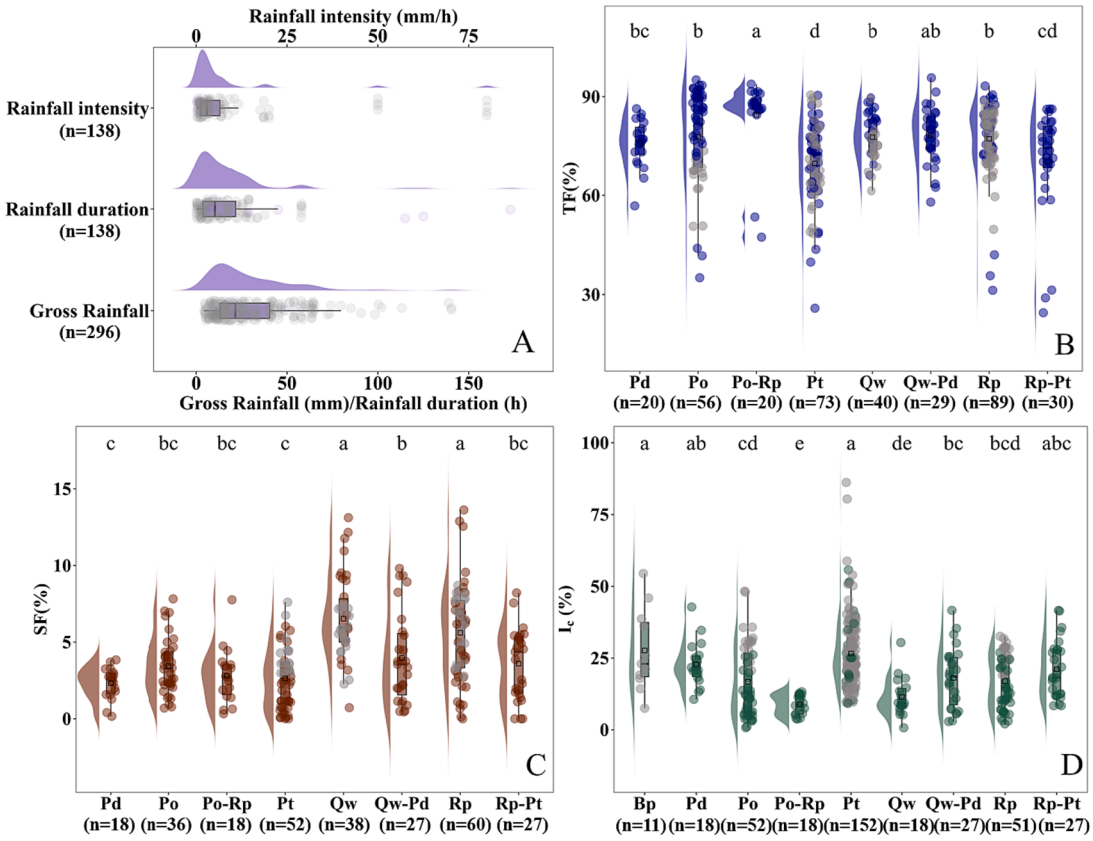

Fig. 3. Characteristics of event size, event intensity and event duration in the study area (A). Distribution of the percentages of TF(B), SF(C), and I_c (D) of different types of stands. Box plots represent the kernel density distribution. Significant differences were indicated by different lowercase letters. At the bottom of the figures represent the total number of rainfall events in different stands for observation and data mining. Bp: *Betula platyphylla.* Data are from our field observation and data mining. Field observation are presented in colors and mined data in gray.

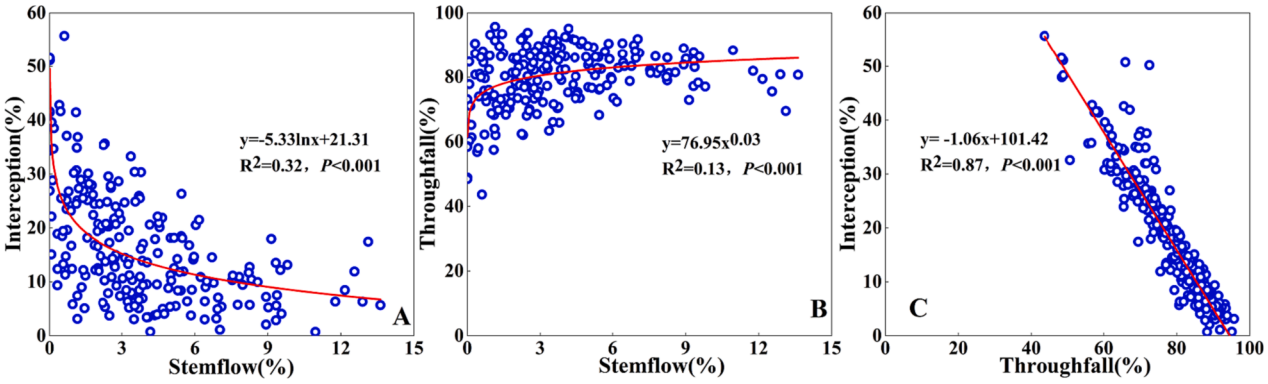

Fig. 4. Regression among the percentages of TF (A), SF (B) and I_c (C). Data sources include field observations and data mining from literatures.

Table 3
Comparison of TF, SF, I_c and its percentages of GR in different types of stands.

Classification Criteria	Groups	TF (mm)	SF (mm)	I_c(mm)	TF/GR(%)	SF/GR(%)	I_c/GR(%)
Origin	Plantation	187.5 ± 12.6 a	9.7 ± 4.1 a	24.8 ± 8.1b	79.7 ± 5.3 a	4.1 ± 1.6 a	10.6 ± 5.5 a
	Natural	191.0 ± 6.1 a	7.5 ± 2.2b	33.2 ± 6.8 a	81.2 ± 2.6 a	4.5 ± 1.8 a	12.8 ± 4.2 a
Species composition	Coniferous	187.0 ± 14.8 a	7.7 ± 2.6 a	28.1 ± 16.3 a	79.5 ± 6.3 a	3.3 ± 1.1b	11.9 ± 6.9 a
	Broad-leaved	190.6 ± 5.3 a	9.9 ± 4.3 a	27.5 ± 9.9 a	81.1 ± 2.3 a	5.1 ± 1.8 a	10.8 ± 4.4 a
	Mixed	186.7 ± 13.1 a	8.8 ± 1.8 a	26.0 ± 9.6 a	79.4 ± 5.6 a	3.7 ± 0.8 ab	11.0 ± 4.1 a

Note: Values are given as mean ± standard error. Significant differences were indicated by different lowercase letters. The same below. Data were obtained from field observations and data mining.

Table 4
The rainfall thresholds (mm) of TF and SF in different types of stands.

Classification criteria	Groups	TF	SF
Origin	Plantation	2.2 ± 0.4 a	3.9 ± 2.5 a
	Natural	1.8 ± 0.5b	2.8 ± 2.0 a
Species composition	Conifers	2.6 ± 1.1 a	3.5 ± 2.6 a
	Broad-leaved	1.8 ± 0.5b	3.7 ± 1.8 a
	Mixed	3.0 ± 1.0 a	5.0 ± 1.7 a

Note: Data sources include our field observations and data mining.

3.3. Influential factors on the rainfall partitioning components

Despite of the similarities in the hydrological dynamics across stands, significant influences of the stand features were found in the amount of the GRP components.

Hierarchical multiple regression analysis showed that R^2 of model improved effectively when DBH, TH, CA and other structural factors were included in each rainfall partitioning component (TF, SF and I_c) model. Species identity was not statistically significant in any GPR component (Table 5).

TF was universally dominated by the environmental factors, especially by P, D and IEI which explained a total of 88.9 % and 93.7 % TF variation in natural forests and plantations (Fig. 5A &D), respectively. The dominance of P was also found in SF in both forest types (Fig. 5B &E). Compared to TF, SF was increasingly influenced by the biotic factors. TH and TD accounted 26.4 % and 13.5 % of SF variations in natural forest and plantation stands, respectively. Moreover, stand attributes, such as CA, DBH and species, were comparatively more important in plantations (Fig. 5E) than in the natural forests (Fig. 5B).

Drastic differences were found in the influencing factors on I_c between the two types of the stands (Fig. 5C &F). Stand attributes combined to explain 62.3 % of I_c in plantations (Fig. 5F), while only 36.5 % of I_c in natural forest stands (Fig. 5C). Among different stand attributes, species identity was the most influential factor for plantation I_c but only counted 22.2 % of I_c variation. In both type of forests, structural factors weighed over species variances in influencing I_c.

In the comparison from the perspective of stand species composition (Fig. 6), environmental factors were still found to dominate TF of all types of stands. The importance of stand attributes grew in their influence on SF (Fig. 6B, E &H), especially in the broadleaf forest (Fig. 6E). When it came to the influence on I_c, the influences of stand attributes increased substantially across all stand types with an accumulative relative influence over 46.0 %, especially in the coniferous stands (accumulative relative influence = 71.5 %). Species identity ranked the second in its importance in explaining I_c in coniferous and mixed stands (Fig. 6C & I). When compared with the environmental factors in terms of relative importance, the total influences of stand attributes became increasingly important following the order of on TF, SF and I_c, irrespective of forest types and species (Table 5 and Fig. S2). Stand structural factors triumph species identity in their explanatory power except for the mixed stands (Fig. 6I).

The partial dependence plots derived from BRT analysis revealed the positive stepwise relationship of I_c with both rainfall amount and canopy area (Fig. 7G and Fig. 7H). By contrast, tree height, DBH and stand density were found to have negative relationships with I_c. The highest I_c would be reached in the stands with the tipping point of TH = 7.5 m (Fig. 7F), DBH = 11.6 cm (Fig. 7I) and TD = 1250 trees·ha^{-1} (Fig. 7J). To further test these tipping points, we compared the correlation variations of the relevant stand structures between the contrasting conditions of the tipping points (Fig. 8). The positive correlation of TH with both LAI and CA changed to negative and non-significant, respectively as TH surpassed 7.5 m (Fig. 8A and B). The DBH-CA correlation changed from positive to negative as DBH exceeded 11.6 cm (Fig. 8C and D). Similarly, TD was negatively correlated with CA and none-correlated with LAI

Table 5
Hierarchical multiple regression analysis for the rainfall partitioning component.

Factors	TF				SF				I_c			
	Without considered		Considered		Without considered		Considered		Without considered		Considered	
	Coefficient	Standardized coefficient	Coefficient	Standardized coefficient	Coefficient	Standardized coefficient	Coefficient	Standardized coefficient	Coefficient	Standardized coefficient	Coefficient	Standardized coefficient
intercept	18.365**		24.743		1.121**		−0.181		2.705		−2.474	
Species	0.120	0.018	−0.089	−0.013	−0.005	−0.010	0.063	0.134	0.055	0.066	0.158	0.188
DBH			−0.391	−0.041			−0.005	−0.007			**0.449****	0.373
TH			0.364	0.046			**0.187****	0.332			**−0.530****	−0.528
CA			−0.065	−0.019			−0.014	−0.056			0.041	0.095
TD			−0.002	−0.045			0.000	0.098			**0.001***	0.231
LAI			−0.167	−0.010			−0.158	−0.135			0.378	0.182
R^2	0.000		0.003		0.000		0.102		0.004		0.173	
F	0.065		0.085		0.019		**3.293***		0.775		**6.036****	
ΔR^2	0.000		0.002		0.000		0.102		0.004		0.169	
ΔF	0.065		0.090		0.019		**3.947***		0.775		**7.062****	

Note: Without considered means that the factors of stand structure are not taken into considered. Significant relationships are highlighted in bold ($p < 0.05$).

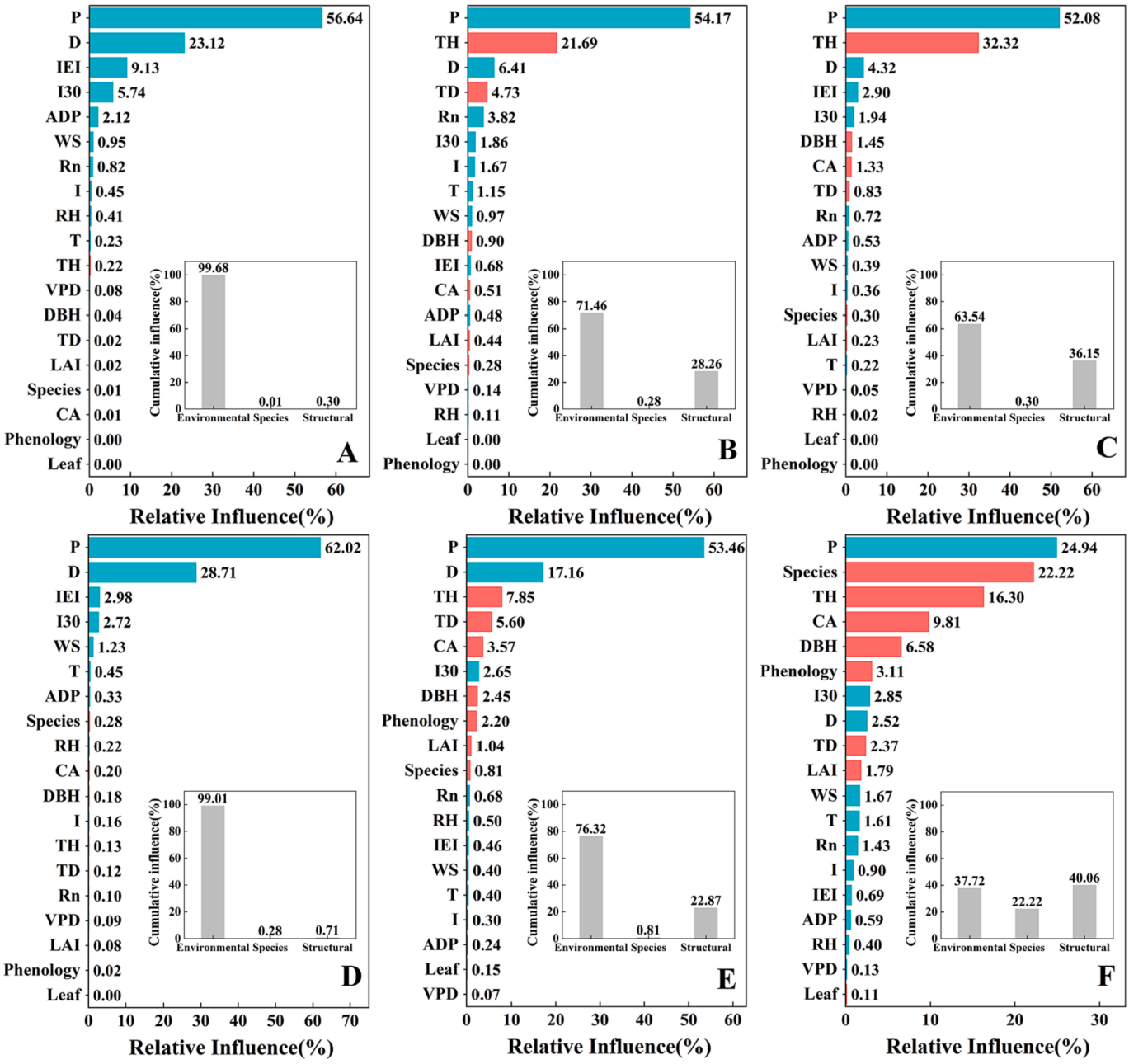

Fig. 5. Relative contribution of individual biotic (pink) and environmental (blue) factors to TF, SF, and I_c in the natural forests (A-C) and plantations (D-F), respectively. Abbreviations of the influencing factors were given in Table 2. Cumulative influences of environmental, species, and structural factors were embedded in the lower right corner of the corresponding subfigures. (For interpretation of the references to colour in this figure legend, the reader is referred to the web version of this article.)

when TD <1250 trees·ha^{-1}. By contrast, TD demonstrated positive relationship with both CA and LAI when TD >1250 trees·ha^{-1} (Fig. 8E and F).

3.4. General predictive models of GRP components for the Loess area

Based on the BRT results, predictive models of rainfall partition components were built based on the most influential factors with the cumulative explanatory power over 70 % (Table 6). The comparison between our BRT formulas and other studies showed that our formula captured well the observatory GRP budgets (Fig. 9, Table S4). The performance of the BRT predictive model is improved compared with other linear and power functions (Table S4).

4. Discussion

Identification of the driving factors of the GRP fluxes is of great importance for estimating hydrological budget in diverse vegetated ecosystems. We have the advantage of exploring the effects of structural traits in forests of different stand attributes under similar driving forces, including the geographic vicinity and hydrometeorological background. Meanwhile, we also included other studies that encompass large spatial and temporal variability. Therefore, our results would be robust in analyzing the structural traits across stands. Except for the mixed stands (Fig. 6I), the cumulative influences of structural factors still triumph over that of the species identity. Therefore, it would be reasonable to say that our hypothesis applies in most circumstances. Based on this understanding, we build effective quantitative relationships between GRP

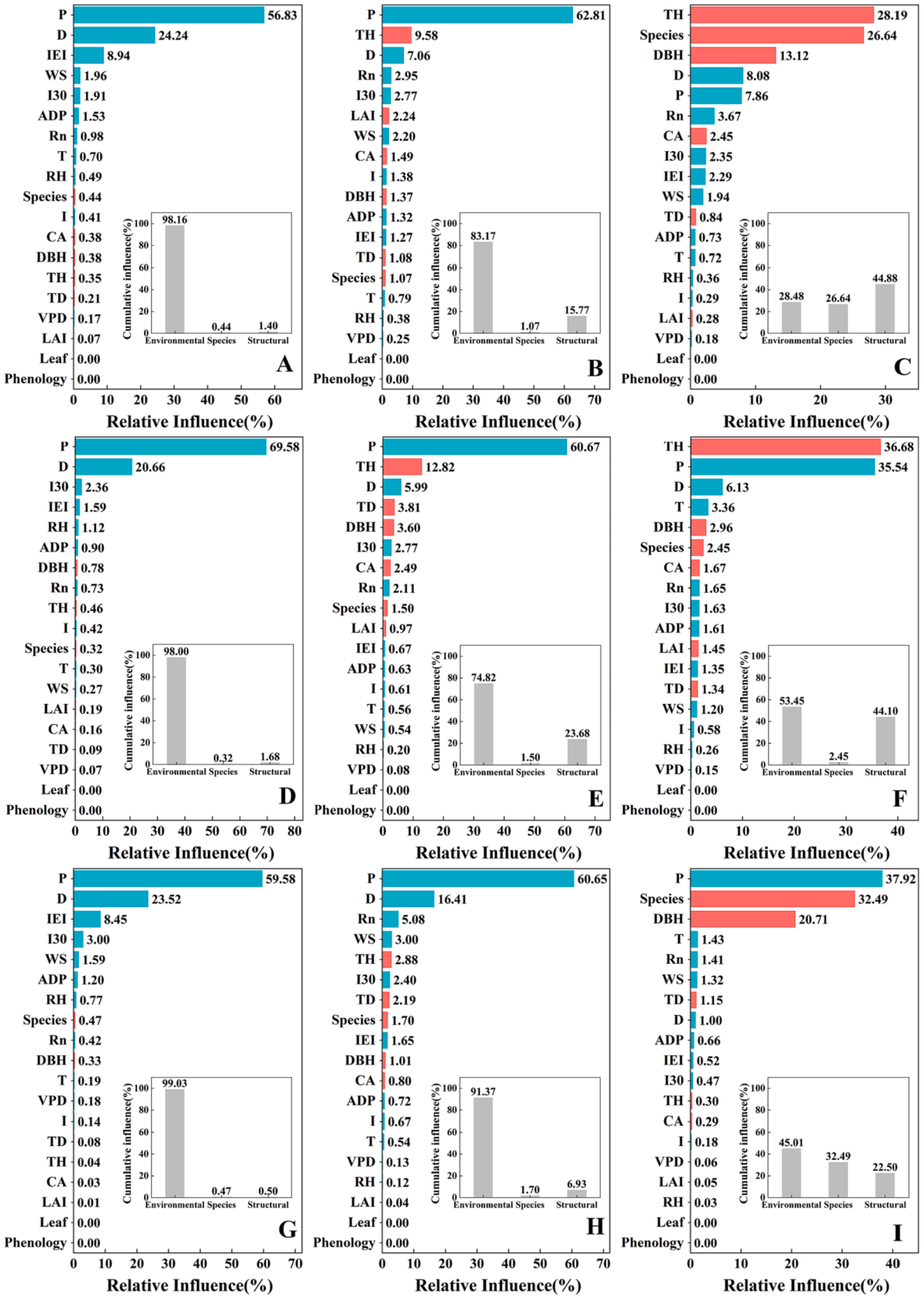

Fig. 6. Relative contribution of individual biotic (pink) and environmental (blue) factors to TF, SF, and I_c in coniferous (A-C), broad-leaved (D-F), and mixed (G-I) forests, respectively. Abbreviations of the influencing factors are given in Table 2. Cumulative influences of environmental, species, and structural factors were embedded in the lower right corner of the corresponding subfigures. (For interpretation of the references to colour in this figure legend, the reader is referred to the web version of this article.)

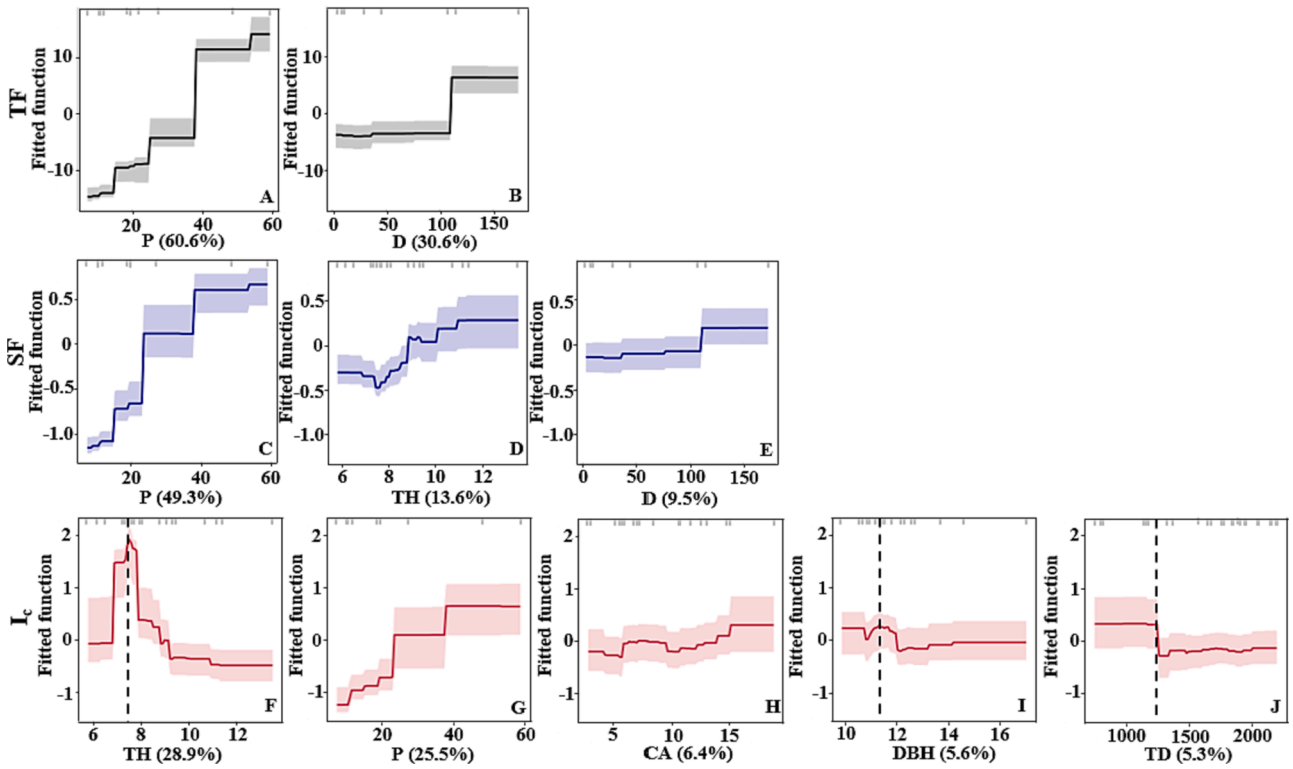

Fig. 7. BRT-model-derived partial dependence of TF (black), SF (darkblue), and I_c (crimson) on influential factors (exceeding a cumulative RI of 70%). Gray rug plots at the top x-axis demonstrate the percentile distribution of the response variables. The shaded zones represent the 95% confidence intervals based on 500 bootstrap replicates. The vertical black broken line in F、I and J represents the tipping points for TH、DBH and TD, respectively. RI scores are given in the x-axis for each variable. Refer to Table 2 for variable abbreviations in the figure.

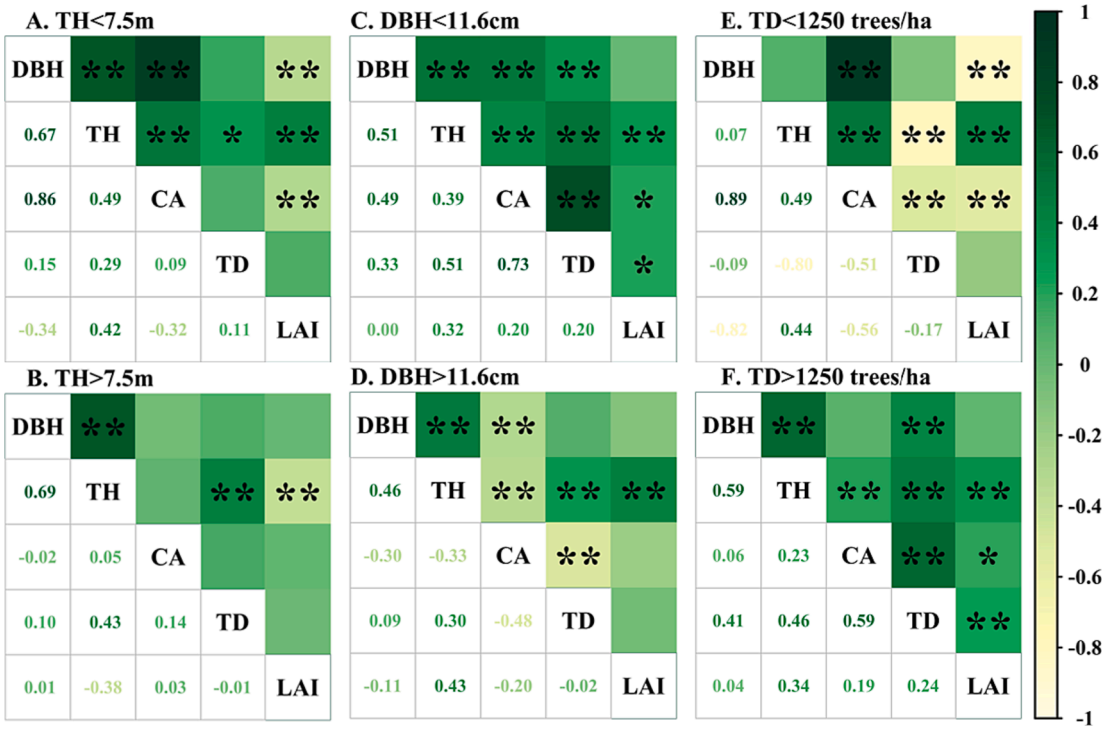

Fig. 8. Correlation matrix of structural factors under the conditions of tipping points of TH (A & B), DBH (C & D) and density (E & F).

Table 6
Predictive models of TF, SF and I_c in the BRT model.

Rainfall components (mm)	Indicator	P	Coefficient	R^2	P
TF	Intercept	<0.001***	−2.020	0.966	<0.001
	P	<0.001***	0.849		
	D	<0.001***	0.016		
SF	Intercept	<0.001***	−1.529	0.754	<0.001
	P	<0.001***	0.051		
	D	0.828	−0.001		
	TH	<0.001***	0.163		
I_c	Intercept	0.141	−1.051	0.461	<0.001
	P	<0.001***	0.066		
	DBH	<0.001***	0.311		
	TH	0.006**	−0.209		
	CA	0.252	0.023		
	TD	0.226	0.001		

Note: TF: Throughfall (mm); SF: Stemflow (mm); I_c: Interception (mm); P: Precipitation (mm); D: Rainfall duration (h); TH: Tree height (m); CA: Canopy area (m^2); DBH: Diameter at breast height (cm); TD: Stand density (trees·ha^{-1}).

components and the influential factors in the same region.

4.1. *Residence of rainfall on trees determine the relative importance of precipitation vs. structure attributes on rainfall partitioning*

Previous studies have observed greater influences of the meteorological variables, such as rainfall amount/duration/intensity, VPD *etc.* on rainfall partitioning compared with tree structure traits (Del Campo et al., 2018; Yang et al., 2019; Zhang et al., 2023b). Similarly, we found that rainfall attributes were influential for all GRP components. However, we discovered a clear pattern that the explanatory power of the rainfall attributes gradually decreases in the sequence of TF, SF and I_c (Figs. 5 & 6). Canopy serves as the interface of rainfall interactions and thus intercept rainfall throughout the event. Therefore, canopy attributes, such as height, leaf morphology, branch angles and canopy hydrophobicity *etc.* determine the canopy capacity in holding rainfall and thus have great influences on the amount of I_c. Another source of intercepted rainfall is from tree trunks where barks and branches can absorb and hold rainwater. Significant differences were observed between bark types in other field studies (Van Stan et al., 2016; Zhang et al., 2020). The variation in hydro-physical properties of bark (Ilek et al., 2019) was also found between organs of individual trees (Ilek et al., 2021). Therefore, the heterogeneity of stand structures presides over the variation of I_c across different stands even under same rainfall input background.

Different from I_c, TF generation can be divided into two phases. Before the point of reaching full canopy capacity, TF mainly either directly pass through the canopy gaps as free throughfall or indirectly through the formation of some preferential dripping points (Fathizadeh et al., 2021) and drops splashing from the canopy (Su et al., 2022). Canopy architectures determine the formation of flow paths (Nanko et al., 2022). Leaves mostly form short-residence flow paths due to their hydrophobic-prone nature (Ginebra-Solanellas et al., 2020). Therefore, the leaf-volume is crucial to the amount of short-residence flow-paths. Consequently, dense canopy, either due to stand density, leaf biomass or branch overlap, would increase the canopy water-holding capacity and intercept rainfall, thus hinder the TF generation. At the second stage, the canopy reservoir fills as rainfall progresses. Our observed TF/GRP increase implies the formation of more drainage pathways as the canopy gets fuller (Rodrigues et al., 2022). Beyond full canopy capacity, most observation reflect direct free fall or those quick-pass water although the water drained from the canopy still constitute a small fraction of TF (Germer et al., 2005; Gerrits et al., 2010). Therefore, the influences of stand structures should be further limited after the canopies reach their full capacity and TF mainly depends on the rainfall conditions. Consequently, rainfall attributes dominate the amount of throughfall.

Compared with TF, SF generates as the full canopy and bark storage promotes water routing increasingly through the stem flow path to the forest floor (Levia and Germer, 2015; Rodrigues et al., 2022). Moreover, branch routes mostly constitute medium- and longer-residence flow paths (Nanko et al., 2022). Therefore, SF threshold is more pronounced than TF. SF has the longest travelling distance along the branches and stem; therefore, most influenced by the tree and stand structures. Individual-specific tree characteristics highly influenced its generation, causing high variances among individuals within the stand (Fig. 3B). Consequently, the initiation values of SF failed to show significant differences among different types of stands (Table 4). Moreover, at full capacity of canopy reservoir, the drainage maintained stably at the maximum value, reducing the intraspecies variances. Therefore, the total SF depth was similar among different forest types (Table 3). This causality relationship among TF, SF and I_c resulted in similar GRP across stands. It also explained the varied importance of structure attributes for GRP components.

4.2. *Stand structural attributes were strong predictors for GRP*

Except for the mixed stand (Fig. 6I), we found higher cumulative explanatory power of structural factors than species across different types of forest (Figs. 5 & 6). This finding contrasts with previously studies where species identity has long been regarded a pronounced factor on GRP (Baptista et al., 2018; Cano-Arboleda et al., 2022; Tonello et al., 2021). The disparities might rise from the fact that most of strong

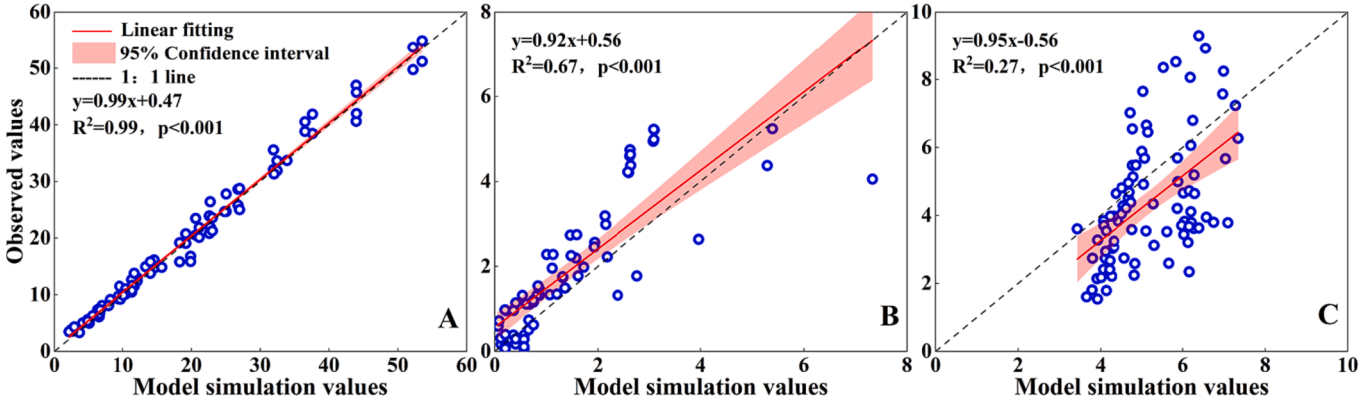

Fig. 9. Relationship between simulated values and field observed values of BRT model. A, B and C represent TF, SF and I_c, respectively. The comparison between the modeled and observation values were derived from the test dataset.

identity effects are usually intertwined with the structural features, such as dense crown structure, distinct leaf morphology, overlapping branches and foliage, in the comparison of stands of different species-composition (Cano-Arboleda et al., 2022). Our study successfully separating the structural traits from species identity, and identifies the pure influence of species identity, such as in cases of mixed stands (Fig. 6I). The ecosystem can function higher/lower in a mixed stand than in monoculture stands either because of the selection or the complementarity effects (van der Plas et al., 2016; Zhang et al., 2022). The complex species interaction can be more prominent in mixed stands than in pure stands (Fig. 6I V.S. 6C&I), leading to a higher influence of species than the cumulative influences of structure factors in the mixed stands (Fig. 6I). The pure species influences were high also in SF and TF of plantation and coniferous stands (Fig. 5F and Fig. 6C) but the cumulative influence of structural traits still prevail. Moreover, structural attributes would change dramatically during the life span, which makes it even less accountable to attribute GRP to species identity. Therefore, considering the predominant role of structural attributes in most cases, focusing on species identity may keep the evaluation of individual features within a certain range instead of specific values and cause errors in the modelling process.

Among the structural factors, we found TH and DBH to be more influential than CA and LAI in many cases (Figs. 5 & 6). Canopy roughness length influences the water and energy flux between the stand and the atmosphere (Bonan et al., 2021; Fan et al., 2023). Moreover, the large and high trees are more exposed to atmospheric advection which would promote the trunk and canopy storage evaporation which otherwise would have formed drainage along the canopy and stem routes. Meanwhile, the shorter and smaller trees are sheltered from energy advection between inside and outside of the stands, diminishing tree body evaporative loss (Ringgaard et al., 2014). Therefore, variations of tree height and size are likely to complicate the correlations between GRP components and hydrometeorological factors, e.g. rainfall characteristics, VPD, and wind speed (Brauman et al., 2010; Dong et al., 2020), strengthening the influence of structural attributes on their GRP (Francis et al., 2022; Jiang et al., 2019).

We found that the trade-off between structural traits (Fig. 8) is influencing the relationship between GRP components and structural traits (Fig. 7). Resources limitation would lead to growth competition, which directly impact stand structural attributes. The phytoeconomic spectrum can cause trade-offs in the characteristics of adjacent individuals (Wang et al., 2022). Therefore, as the influences of structure attributes of different individuals merge to form stand character, individual performance associated with species identity would diminish as the observational scale increases. Such structure dynamics would have functional consequences. For example, the influence of individual structure on transpiration is weakened during scale extension, and the influence of group structure is more evident (Li et al., 2022; Zhang et al., 2023a). Therefore, as SF and I_c are strongly rely on the cumulative influences of stand structural factors (Figs. 5 & 6), the similarities in stand structures, such as DBH and LAI (Fig. 2C &D), would partially count for the lack of the differences of GRP components among stands of different species compositions (Table 3). Furthermore, this study successfully established general formula to describe GRP partitioning components of plantation stands across the region with structure factors accounted most of the influential factors (Fig. 9 and Table 6). For other regions with different rainfall regimes, our parameter values might not be applicable but our approach might be viable.

It should be noted that our statement of structural attributes over species identity over GRP is per growing season. During the growing season, the canopy features are relevant stable and the GRP process is more a physical process. Therefore, the species-specific biotic process, e.g. canopy phenology does not involve. Seasonally variable biological activity and canopy phenology cause strong variations in canopy surface and its function in GRP (Anna and Wojciech, 2018; Blume et al., 2022; Michalzik et al., 2016; Nanko et al., 2022; Zhang et al., 2022). Moreover, the differences of canopy between coniferous forest and broadleaved forest in non-growing season makes large differences of GRP during the non-growing season (Ouyang et al., 2021). In addition, species diversity has also been proved to have indirect impact on GRP. Findings from (Barbier et al., 2009; Frischbier and Wagner, 2015; Zabret et al., 2018) stresses the importance of leaf phenology in studies on rainfall partitioning. Therefore, the comparative importance of species identity and stand structures worth further exploration when it comes to the transition period between the dormant and the growing season.

4.3. Implications of stand configurations for eco-restoration

Predictions of altered rainfall regimes have brought up the exploration over how to balance socio-economic water demands with ecosystem hydrological processes and functioning of these plantations (Attarod et al., 2015; Davis et al., 2015; Lian et al., 2022). Multiple previous studies have established linear relationships of GRP components with the single stand structural variable (Brantley et al., 2019; Niu et al., 2023). However, large uncertainty remains in characterizing forest stand structures using the single stand structural variable (Angela et al., 2015). Moreover, most of them are species-specific or site-specific, hampering the wide applications of these relationships due to the variations in stand configurations and varied species physiologic characteristics (Exler and Moore, 2022; Wu et al., 2021; Zhao et al., 2023). Therefore, determining the priorities of importance in species and stand structures would facilitate the establishment of effective predictive models for GRP components and applicable for estimation at larger scales.

Our results suggest that species-dependent selections would over simplify the forest stand water balance dynamics over time. Instead, researchers can catalogue the ecohydrological properties of stand structural attributes to inform decision-makers and with the species growth trajectory to formulate the management plans for maintaining a sustainable structure affordable by local water resources.

Species configurations in eco-restoration projects usually are not considered in stand structural traits pertaining to ecohydrological functions. Our results highlight the importance of that structural configuration for advancing the modelling of eco-restoration projects' roles on ecohydrological processes. Our BRT models have the potential to estimate the GRP components across the Loess area (Table 6). Therefore, the application of BRT modelling would be a practical tool with input of commonly forest inventories that can allow the evaluation of GRP over large plantation areas to optimize forest and water managements.

5. Conclusions

Forest stands with different configurations demonstrate consistent hydrological dynamics regardless of tree species composition or stand origin. Stands of different types, by origin or species composition, rarely have significant differences in throughfall (TF) in an arid region. However, stand origins or species compositions could have significantly different stemflow (SF) or canopy interception (I_c). The BRT analysis revealed that TF was dominant by rainfall attributes. However, SF and I_c increasingly rely on structural attributes as the rain water residence time increased. The BRT models developed based on precipitation and structural traits captured the stand-scale TF and SF better than I_c across variable stands on the Loess Plateau. Therefore, we conclude that structural factors play a predominant role in determining GRP process during the growing season.

Our study highlights the influences of stand structures in regulating the SF and I_c of GRP. Estimating GRP should consider different phenological phases when species differences might play a significant role. This present study contributes to a more holistic understanding of GPR temporal variations for better modeling GRP at the regional scale. Finally, using a single reference value to represent certain species or

forest types in large-scale water balance evaluation may cause large errors. A comprehensive understanding of the influence variable on GRP is needed to the effects of the plantations on watershed water cycles. Therefore, our findings are helpful for improving ecohydrological prediction models that are critical for the implementation of large-scale eco-restoration projects.

CRediT authorship contribution statement

Xu Hu: Data curation, Methodology, Formal analysis, Visualization, Writing – original draft, Writing – review & editing. **Zhaoqi Fu:** Data curation, Writing – original draft, Writing – review & editing. **Ge Sun:** Methodology, Formal analysis, Writing – review & editing. **Biao Wang:** Data curation, Writing – review & editing. **Keyan Liu:** Data curation, Writing – review & editing. **Churui Zhang:** Data curation, Writing – review & editing. **Lu Han:** Formal analysis, Visualization, Writing – review & editing. **Lixin Chen:** Methodology, Formal analysis, Visualization, Writing – original draft, Writing – review & editing. **Zhiqiang Zhang:** Methodology, Writing – original draft, Writing – review & editing.

Declaration of competing interest

The authors declare that they have no known competing financial interests or personal relationships that could have appeared to influence the work reported in this paper.

Data availability

Data will be made available on request.

Acknowledgements

This research was funded by the National Key Research and Development Program of China (2022YFF1302501) and National Natural Science Foundation of China (41977149 and 41877152). The authors also greatly appreciate the review effort by the anonymous reviewers.

Appendix A. Supplementary data

Supplementary data to this article can be found online at https://doi.org/10.1016/j.jhydrol.2024.130671.

References

Adane, Z.A., Gates, J.B., 2015. Determining the impacts of experimental forest plantation on groundwater recharge in the Nebraska sand hills (USA) using chloride and sulfate. Hydrogeol. J. 23 (1), 81–94. https://doi.org/10.1007/s10040-014-1181-6.

An, J.X., Gao, G., Yuan, C.Y., Pinos, J., Fu, B.J., 2022. Inter- and intra-event rainfall partitioning dynamics of two typical xerophytic shrubs in the Loess Plateau of China. Hydrol. Earth Syst. Sci. 26 (14), 3885–3900. https://doi.org/10.5194/hess-26-3885-2022.

Angela, M.A., María, G.S., Antonio, D.D.C., 2015. Light detection and ranging for implementing water-oriented forest management in a semiarid sub-catchment (Valencia, Spain). Clean - Soil Air Water 43 (11), 1488–1494. https://doi.org/10.1002/clen.201400871.

Anna, K.I., Wojciech, W., 2018. Variability in the wettability and water storage capacity of common oak leaves (Quercus robur L.). Water 10 (6), 695. https://doi.org/10.3390/w10060695.

Attarod, P., Sadeghi, S.M.M., Pypker, T.G., Bagheri, H., Bagheri, M., Bayramzadeh, V., 2015. Needle-leaved trees impacts on rainfall interception and canopy storage capacity in an arid environment. New Forests. 46 (3), 339–355. https://doi.org/10.1007/s11056-014-9464-2.

Baptista, M.D., Livesley, S.J., Parmehr, E.G., Neave, M., Amati, M., 2018. Variation in leaf area density drives the rainfall storage capacity of individual urban tree species. Hydrol. Process. 32 (25), 3729–3740. https://doi.org/10.1002/hyp.13255.

Barbier, S., Balandier, P., Gosselin, F., 2009. Influence of several tree traits on rainfall partitioning in temperate and boreal forests: a review. Ann. for. Sci. 66 (6), 602. https://doi.org/10.1051/forest/2009041.

Blume, T., Schneider, L., Güntner, A., 2022. Comparative analysis of throughfall observations in six different forest stands: influence of seasons, rainfall- and stand characteristics. Hydrol. Process. 36 (3), e14461 https://doi.org/10.1002/hyp.14461.

Bonan, G.B., Patton, E.G., Finnigan, J.J., Baldocchi, D.D., Harman, I.N., 2021. Moving beyond the incorrect but useful paradigm: reevaluating big-leaf and multilayer plant canopies to model biosphere-atmosphere fluxes - a review. Agric. For. Meteorol. 306, 108435 https://doi.org/10.1016/j.agrformet.2021.108435.

Brantley, S.T., Miniat, C.F., Bolstad, P.V., 2019. Rainfall partitioning varies across a forest age chronosequence in the southern Appalachian Mountains. Ecohydrology 12 (4), e2081. https://doi.org/10.1002/eco.2081.

Brauman, K.A., Freyberg, D.L., Daily, G.C., 2010. Forest structure influences on rainfall partitioning and cloud interception: A comparison of native forest sites in Kona, Hawai'i. Agric. For. Meteorol. 150 (2), 265–275. https://doi.org/10.1016/j.agrformet.2009.11.011.

Cano-Arboleda, L.V., Villegas, J.C., Restrepo, A.C., Quintero-Vallejo, E., 2022. Complementary effects of tree species on canopy rainfall partitioning: New insights for ecological restoration in Andean ecosystems. For. Ecol. Manag. 507, 119969 https://doi.org/10.1016/j.foreco.2021.119969.

Davis, J., O'Grady, A.P., Dale, A., Arthington, A.H., Gell, P.A., D.Driver, P., Bond, N., Casanova, M., Finlayson, M., Watts, R. J., Capon, S.J., Nagelkerken, I, Tingley, R., Fry, B., Page, T.J., Specht, A., 2015. When trends intersect: The challenge of protecting freshwater ecosystems under multiple land use and hydrological intensification scenarios. Sci. Total Environ. 534, 65-78.

de Lima, J.A., Tonello, K.C., 2023. Rainfall partitioning in Amazon forest: implications of reduced impact logging for hydrological processes. Agric. For. Meteorol. 337, 109505 https://doi.org/10.1016/j.agrformet.2023.109505.

Del Campo, A.D., González-Sanchis, M., Lidón, A., Ceacero, C.J., García-Prats, A., 2018. Rainfall partitioning after thinning in two low-biomass semiarid forests: impact of meteorological variables and forest structure on the effectiveness of water-oriented treatments. J. Hydrol. 565, 74–86. https://doi.org/10.1016/j.jhydrol.2018.08.013.

Ding, W.B., Wang, F., Han, J.Q., Ge, W.Y., Cong, C.Y., Deng, L.Q., 2021. Throughfall and its spatial heterogeneity in a black locust (Robinia pseudoacacia) plantation in the semi-arid loess region, China. J. Hydrol. 602, 126751 https://doi.org/10.1016/j.jhydrol.2021.

Dong, L.L., Han, H.R., Kang, F.F., Cheng, X.Q., Zhao, J.L., Song, X.S., 2020. Rainfall partitioning in Chinese Pine (Pinus tabuliformis Carr.) Stands at three different ages. Forests 11 (2), 243. https://doi.org/10.3390/f11020243.

Elith, J., Leathwick, J.R., Hastie, T., 2008. A working guide to boosted regression trees. J. Anim Ecol. 77 (4), 802–813. https://doi.org/10.1111/j.1365-2656.2008.01390.x.

Exler, J.L., Moore, R.D., 2022. Quantifying throughfall, stemflow and interception loss in five vegetation communities in a maritime raised bog. Agric. For. Meteorol. 327, 109202 https://doi.org/10.1016/j.agrformet.2022.109202.

Fan, C., Jiao, L., Lu, N., Li, M.T., Li, Z.S., Keyimu, M., Zhang, L.W., Wang, H., 2023. Disentangling the independent and interacting impacts of biophysical factors on the transpiration of a black locust (Robinia pseudoacacia) plantation in the semiarid Loess Plateau, China. Land Degrad. Dev. 34 (6), 1767–1777. https://doi.org/10.1002/ldr.4567.

Fathizadeh, O., Sadeghi, S.M.M., Pazhouhan, I., Ghanbari, S., Attarod, P., Su, L., 2021. Spatial variability and optimal number of rain gauges for sampling throughfall under single oak trees during the leafless period. Forests 12 (5), 585. https://doi.org/10.3390/f12050585.

Feng, X.M., Fu, B.J., Piao, S.L., Wang, S., Ciais, P., Zeng, Z.Z., Lü, Y.H., Zeng, Y., Li, Y., Jiang, X.H., Wu, B.F., 2016. Revegetation in China's Loess Plateau is approaching sustainable water resource limits. Nat. Clim. Chang. 6 (11), 1019–1022. https://doi.org/10.1038/nclimate3092.

Feng, T.J., Wei, T.X., Saskia, D.K., Zhang, J.J., Bi, H.X., Wang, R.S., Wang, P., 2023. Long-term effects of vegetation restoration on hydrological regulation functions and the implications to afforestation on the Loess Plateau. Agric. for. Meteorol. 330, 109313 https://doi.org/10.1016/j.agrformet.2023.109313.

Forrester, D.I., 2019. Linking forest growth with stand structure: Tree size inequality, tree growth or resource partitioning and the asymmetry of competition. For. Ecol. Manag. 447, 139–157. https://doi.org/10.1016/j.foreco.2019.05.053.

Francis, J.R., Wuddivira, M.N., Farrick, K.K., 2022. Exotic tropical pine forest impacts on rainfall interception: canopy, understory, and litter. J. Hydrol. 609, 127765 https://doi.org/10.1016/j.jhydrol.2022.127765.

Frischbier, N., Wagner, S., 2015. Detection, quantification and modelling of small-scale lateral translocation of throughfall in tree crowns of European beech (Fagus sylvatica L.) And Norway spruce (Picea abies (L.) Karst). J. Hydrol. 522, 228–238. https://doi.org/10.1016/j.jhydrol.2014.12.034.

Gao, G.Y., Ma, Y., Fu, B.J., 2016. Multi-temporal scale changes of streamflow and sediment load in a loess hilly watershed of China. Hydrol. Process. 30 (3), 365–382. https://doi.org/10.1002/hyp.10585.

Germer, S., Elsenbeer, H., Moraes, J.M., 2005. Throughfall and temporal trends of rainfall redistribution in an open tropical rainforest, south-western Amazonia (Rondônia, Brazil). Hydrol. Earth Syst. Sci. 10 (3), 383–393.

Gerrits, A.M.J., Pfister, L., Savenije, H.H.G., 2010. Spatial and temporal variability of canopy and forest floor interception in a beech forest. Hydrol. Process. 24 (21), 3011–3025. https://doi.org/10.1002/hyp.7712.

Ginebra-Solanellas, R.M., Holder, C.D., Lauderbaugh, L.K., Webb, R., 2020. The influence of changes in leaf inclination angle and leaf traits during the rainfall interception process. Agric. for. Meteorol. 285–286, 107924 https://doi.org/10.1016/j.agrformet.2020.107924.

Honda, E.A., Mendonça, A.H., Durigan, G., 2015. Factors affecting the stemflow of trees in the Brazilian Cerrado. Ecohydrology 8 (7), 1351–1362. https://doi.org/10.1002/eco.1587.

Ilek, A., Szostek, M., Kucza, J., Stanek-Tarkowska, J., Witek, W., 2019. The water absorbability of beech (Fagus sylvatica I.) and fir (Abies alba mill.) organic matter in the forest floor. Ann. For. Res. 52 (1) https://doi.org/10.15287/afr.2018.1161.

Ilek, A., Van Stan, J.T., Morkisz, K., Kucza, J., 2021. Vertical variability in bark hydrology for two coniferous tree species. Front. For. Glob. Change. 4 https://doi.org/10.3389/ffgc.2021.687907.

Jia, X.X., Shao, M.A., Zhu, Y.J., Luo, Y., 2017. Soil moisture decline due to afforestation across the Loess Plateau, China. J. Hydrol. 546, 113–122. https://doi.org/10.1016/j.jhydrol.2017.01.011.

Jian, S.Q., Zhao, C.Y., Fang, S.M., Yu, K., 2015. Effects of different vegetation restoration on soil water storage and water balance in the Chinese Loess Plateau. Agric. For. Meteorol. 206, 85–96.

Jiang, M.H., Lin, T.C., Shaner, P.L., Lyu, M.K., Xu, C., Xie, J.S., Lin, C.F., Yang, Z.J., Yang, Y.S., 2019. Understory interception contributed to the convergence of surface runoff between a Chinese fir plantation and a secondary broadleaf forest. J. Hydrol. 574, 862–871. https://doi.org/10.1016/j.jhydrol.2019.04.088.

Levia, D.F., Germer, S., 2015. A review of stemflow generation dynamics and stemflow-environment interactions in forests and shrublands. Rev. Geophys. 53 (3), 673–714. https://doi.org/10.1002/2015RG000479.

Li, J.L., Chen, X.P., Niklas, K.J., Sun, J., Wang, Z.Y., Zhong, Q.L., Hu, D.D., Cheng, D.L., 2022. A whole - plant economics spectrum including bark functional traits for 59 subtropical woody plant species. J. Ecol. 110 (1), 248–261. https://doi.org/10.1111/1365-2745.13800.

Li, X., Xiao, Q.F., Niu, J.Z., Dymond, S., van Doorn, N.S., Yu, X.X., Xie, B.Y., Lv, X.Z., Zhang, K.B., Li, J., 2016. Process-based rainfall interception by small trees in Northern China: the effect of rainfall traits and crown structure characteristics. Agric. For. Meteorol. 218–219, 65–73. https://doi.org/10.1016/j.agrformet.2015.11.017.

Lian, X., Zhao, W.L., Gentine, P., 2022. Recent global decline in rainfall interception loss due to altered rainfall regimes. Nat. Commun. 13 (1) https://doi.org/10.1038/s41467-022-35414-y.

Lima, W.P., Laprovitera, R., Ferraz, S.F.B., Rodrigues, C.B., Silva, M.M., 2012. Forest plantations and water consumption: a strategy for hydrosolidarity. Int. J. For. Res. 2012, 1–8. https://doi.org/10.1155/2012/908465.

Ma, C.K., Li, X.D., Luo, Y., Shao, M.A., Jia, X.X., 2019. The modelling of rainfall interception in growing and dormant seasons for a pine plantation and a black locust plantation in semi-arid Northwest China. J. Hydrol. 577, 123849.

Magliano, P.N., Whitworth-Hulse, J.I., Baldi, G., 2019. Interception, throughfall and stemflow partition in drylands: Global synthesis and meta-analysis. J. Hydrol. 568, 638–645. https://doi.org/10.1016/j.jhydrol.2018.10.042.

Michalzik, B., Levia, D.F., Bischoff, S., Nathe, K., Richter, S., 2016. Effects of aphid infestation on the biogeochemistry of the water routed through European beech (Fagus sylvatica L.) saplings. Biogeochemistry 129 (1–2), 197–214. https://doi.org/10.1007/s10533-016-0228-2.

Nanko, K., Keim, R.F., Hudson, S.A., Levia, D.F., 2022. Throughfall drop sizes suggest canopy flowpaths vary by phenophase. J. Hydrol. 612, 128144 https://doi.org/10.1016/j.jhydrol.2022.128144.

Niu, X.T., Fan, J., Du, M.G., Dai, Z.J., Luo, R.H., Yuan, H.Y., Zhang, S.G., 2023. Changes of rainfall partitioning and canopy interception modeling after progressive thinning in two shrub plantations on the Chinese Loess Plateau. J. Hydrol. 619, 129299 https://doi.org/10.1016/j.jhydrol.2023.129299.

Ouyang, L., Wu, J., Zhao, P., Li, Y.Q., Zhu, L.W., Ni, G.Y., Rao, X.Q., 2021. Consumption of precipitation by evapotranspiration indicates potential drought for broadleaved and coniferous plantations in hilly lands of South China. Agric. Water. Manag. 252, 106927 https://doi.org/10.1016/j.agwat.2021.106927.

Peterson, B. G., Carl, P., 2019. Performance analytics: econometric tools for performance and risk analysis.

Pflug, S., Voortman, B.R., Cornelissen, J.H.C., Witte, J.P.M., 2021. The effect of plant size and branch traits on rainfall interception of 10 temperate tree species. Ecohydrology 14 (8). https://doi.org/10.1002/eco.2349.

R Core Team, 2022. R: A Language and Environment for Statistical Computing. Http://www.R-Project.Org/.

Ridgeway, G., 2015. Gbm: Generalized Boosted Regression Models.

Ringgaard, R., Herbst, M., Friborg, T., 2014. Partitioning forest evapotranspiration: interception evaporation and the impact of canopy structure, local and regional advection. J. Hydrol. 517, 677–690. https://doi.org/10.1016/j.jhydrol.2014.06.007.

Rodrigues, A.F., Mello, C.R.D., Terra, M.C.N.S., Silva, V.O., Pereira, G.A., Silva, R.A.D., 2019. Soil water content and net precipitation spatial variability in an Atlantic forest remnant. Acta. Sci. Agron. 42, e43518 https://doi.org/10.4025/actasciagron.v42i1.43518.

Rodrigues, A.F., Terra, M.C.N.S., Mantovani, V.A., Cordeiro, N.G., Ribeiro, J.P.C., Guo, L., Nehren, U., Mello, J.M., Mello, C.R., 2022. Throughfall spatial variability in a neotropical forest: have we correctly accounted for time stability? J. Hydrol. 608, 127632 https://doi.org/10.1016/j.jhydrol.2022.127632.

Sadeghi, S.M.M., Gordon, D.A., Van Stan II, J.T., 2020. A global synthesis of throughfall and stemflow, Hydrometeorology. 49-70.

Shinohara, Y., Levia, D.F., Komatsu, H., Nogata, M., Otsuki, K., 2015. Comparative modeling of the effects of intensive thinning on canopy interception loss in a Japanese cedar (Cryptomeria japonica D. Don) forest of western Japan. Agric. for. Meteorol. 214–215, 148–156. https://doi.org/10.1016/j.agrformet.2015.08.257.

Siegert, C.M., Levia, D.F., 2014. Seasonal and meteorological effects on differential stemflow funneling ratios for two deciduous tree species. J. Hydrol. 519, 446–454. https://doi.org/10.1016/j.jhydrol.2014.07.038.

Skhosana, F.V., Thenga, H.F., Mateyisi, M.J., von Maltitz, G., Midgley, G.F., Stevens, N., 2023. Steal the rain: Interception loses and rainfall partitioning by a broad-leaf and a fine-leaf woody encroaching species in a southern African semi-arid savanna. Ecol. Evol. 13 (3), e9868 https://doi.org/10.1002/ece3.9868.

Spencer, S.A., Meerveld, H.J.V., 2016. Double funnelling in a mature coastal British Columbia forest: spatial patterns of stemflow after infiltration. Hydrol. Process. 30 (22), 4185–4201. https://doi.org/10.1002/hyp.10936.

Su, L., Xu, W.T., Zhao, C.M., Xie, Z.Q., Ju, H., 2016. Inter- and intra-specific variation in stemflow for evergreen species and deciduous tree species in a subtropical forest. J. Hydrol. 537, 1–9. https://doi.org/10.1016/j.jhydrol.2016.03.028.

Su, L., Yang, J., Zhao, X., Miao, Y., 2022. Effects of fire on interception loss in a coniferous and broadleaved mixed forest. J. Hydrol. 613, 128425 https://doi.org/10.1016/j.jhydrol.2022.128425.

Sun, J.M., Yu, X.X., Wang, H.N., Jia, G.D., Zhao, Y., Tu, Z.H., Deng, W.P., Jia, J.B., Chen, J.G., 2018. Effects of forest structure on hydrological processes in China. J. Hydrol. 561, 187–199. https://doi.org/10.1016/j.jhydrol.2018.04.003.

Sun, G., Zhou, G.Y., Zhang, Z.Q., Wei, X.H., McNulty, S.G., Vose, J.M., 2006. Potential water yield reduction due to forestation across China. J. Hydrol. 328 (3–4), 548–558. https://doi.org/10.1016/j.jhydrol.2005.12.013.

Sun, G., Wei, X.H., Hao, L., Sanchis, M.G., Hou, Y.P., Yousefpour, R., Tang, R., Zhang, Z.Q., 2023. Forest hydrology modeling tools for watershed management: A review. For. Ecol. Mana. 530, 120755 https://doi.org/10.1016/j.foreco.2022.120755.

Tanaka, N., Levia, D., Igarashi, Y., Yoshifuji, N., Tanaka, K., Tantasirin, C., Nanko, K., Suzuki, M., Kumagai, T., 2017. What factors are most influential in governing stemflow production from plantation-grown teak trees? J. Hydrol. 544, 10–20. https://doi.org/10.1016/j.jhydrol.2016.11.010.

Tonello, K.C., Rosa, A.G., Pereira, L.C., Matus, G.N., Guandique, M.E.G., Navarrete, A.A., 2021. Rainfall partitioning in the cerrado and its influence on net rainfall nutrient fluxes. Agric. For.

van der Plas, F., Manning, P., Allan, E., Scherer-Lorenzen, M., Verheyen, K., Wirth, C., Zavala, M.A., Hector, A., Ampoorter, E., Baeten, L., Barbaro, L., Bauhus, J., Benavides, R., Benneter, A., Berthold, F., Bonal, D., Bouriaud, O., Bruelheide, H., Bussotti, F., Carnol, M., Castagneyrol, B., Charbonnier, Y., Coomes, D., Coppi, A., Bastias, C.C., Muhie Dawud, S., De Wandeler, H., Domisch, T., Finér, L., Gessler, A., Granier, A., Grossiord, C., Guyot, V., Hättenschwiler, S., Jactel, H., Jaroszewicz, B., Joly, F., Jucker, T., Koricheva, J., Milligan, H., Müller, S., Muys, B., Nguyen, D., Pollastrini, M., Raulund-Rasmussen, K., Selvi, F., Stenlid, J., Valladares, F., Vesterdal, L., Zielínski, D., Fischer, M., 2016. Jack-of-all-trades effects drive biodiversity -ecosystem multifunctionality relationships in European forests. Nat. Commun. 7 (1), 11109 https://doi.org/10.1038/ncomms11109.

Van Stan, J.T., Lewis, E.S., Hildebrandt, A., Rebmann, C., Friesen, J., 2016. Impact of interacting bark structure and rainfall conditions on stemflow variability in a temperate beech-oak forest, central Germany. Hydro. Sci. J. 61 (11), 2071–2083. https://doi.org/10.1080/02626667.2015.1083104.

Wang, Z.H., Townsend, P.A., Kruger, E.L., 2022. Leaf spectroscopy reveals divergent inter- and intra-species foliar trait covariation and trait-environment relationships across NEON domains. New Phytol. 235 (3), 923–938. https://doi.org/10.1111/nph.18204.

Wang, Y.H., Yu, P.T., Feger, K.H., Wei, X.H., Sun, G., Bonell, M., Xiong, W., Zhang, S.L., Xu, L.H., 2011. Annual runoff and evapotranspiration of forestlands and non-forestlands in selected basins of the Loess Plateau of China. Ecohydrology 4 (2), 277–287. https://doi.org/10.1002/eco.215.

Wu, X., Shi, W.J., Tao, F.L., 2021. Estimations of forest water retention across China from an observation site-scale to a national-scale. Ecol. Indic. 132, 108274 https://doi.org/10.1016/j.ecolind.2021.108274.

Yang, X.G., Chen, L., Wang, L., Wang, X., Gu, J.L., Qu, W.J., Song, N.P., 2019. Dynamic rainfall-partitioning relationships among throughfall, stemflow, and interception loss by *Caragana intermedia*. J. Hydrol. 574, 980–989. https://doi.org/10.1016/j.jhydrol.2019.04.083.

Yang, J.J., He, Z.B., Feng, J.M., Lin, P.F., Du, J., Guo, L.X., Liu, Y.F., Yan, J.L., 2023. Rainfall interception measurements and modeling in a semiarid evergreen spruce (Picea crassifolia) forest. Agric. For. Meteorol. 328, 109257 https://doi.org/10.1016/j.agrformet.2022.109257.

Yu, M.Z., Zhang, L.L., Xu, X.X., Feger, K.H., Wang, Y.H., Liu, W.Z., Schwärzel, K., 2015. Impact of land-use changes on soil hydraulic properties of Calcaric Regosols on the Loess Plateau, NW China. J. Plant Nutr. Soil Sci. 178 (3), 486–498. https://doi.org/10.1002/jpln.201400090.

Yu, Y., Zhu, J.J., Gao, T., Liu, L.F., Yu, F.Y., Zhang, J.X., Wei, X.H., 2022. Evaluating the influential variables on rainfall interception at different rainfall amount levels in temperate forests. J. Hydrol. 615, 128572 https://doi.org/10.1016/j.jhydrol.2022.128572.

Yuan, C., Gao, G.Y., Fu, B.J., 2016. Stemflow of a xerophytic shrub (Salix psammophila) in northern China: Implication for beneficial branch architecture to produce stemflow. J. Hydrol. 539, 577–588. https://doi.org/10.1016/j.jhydrol.2016.05.055.

Yue, K., De Frenne, P., Fornara, D.A., Van Meerbeek, K., Li, W., Peng, X., Ni, X.Y., Peng, Y., Wu, F.Z., Yang, Y.S., Peñuelas, J., 2021. Global patterns and drivers of rainfall partitioning by trees.

Zabret, K., Sraj, M., 2019. Evaluating the influence of rain event characteristics on rainfall interception by urban trees using multiple correspondence analysis. Water 11 (12), 2659. https://doi.org/10.3390/w11122659.

Zabret, K., Sraj, M., 2021. Relation of influencing variables and weather conditions on rainfall partitioning by birch and pine trees. J. Hydrol. Hydromech. 69 (4), 456–466. https://doi.org/10.2478/johh-2021-0023.

Zabret, K., Rakovec, J., Sraj, M., 2018. Influence of meteorological variables on rainfall partitioning for deciduous and coniferous tree species in urban area. J. Hydrol. 558, 29–41. https://doi.org/10.1016/j.jhydrol.2018.01.025.

Zhang, C., Khan, A., Duan, C.Y., Cao, Y., Wu, D.D., Hao, G.Y., 2023a. Xylem hydraulics strongly influence the niche differentiation of tree species along the slope of a river

valley in a water-limited area. Plant Cell Environ. 46 (1), 106–118. https://doi.org/10.1111/pce.14467.

Zhang, R., Seki, K., Wang, L., 2023b. Quantifying the contribution of meteorological factors and plant traits to canopy interception under maize cropland. Agric. Water Manage. 279, 108195 https://doi.org/10.1016/j.agwat.2023.108195.

Zhang, S.M., Verheyen, K., De Frenne, P., Landuyt, D., 2022. Tree species mixing affects throughfall in a young temperate forest plantation. Agric. For. Meteorol. 327, 109220 https://doi.org/10.1016/j.agrformet.2022.109220.

Zhang, Y.F., Wang, X.P., Hu, R., Pan, Y.X., Paradeloc, M., 2015. Rainfall partitioning into throughfall, stemflow and interception loss by two xerophytic shrubs within a rain-fed re-vegetated desert ecosystem, northwestern China. J. Hydrol. 527, 1084–1095. https://doi.org/10.1016/j.jhydrol.2015.05.060.

Zhang, Y.F., Wang, X.P., Hu, R., Pan, Y.X., 2017. Stemflow volume per unit rainfall as a good variable to determine the relationship between stemflow amount and morphological metrics of shrubs. J. Arid Environ. 141, 1–6. https://doi.org/10.1016/j.jaridenv.2017.02.002.

Zhang, Y.F., Wang, X.P., Pan, Y.X., Hu, R., 2020. Relative contribution of biotic and abiotic factors to stemflow production and funneling efficiency: A long-term field study on a xerophytic shrub species in Tengger Desert of northern China. Agric. For. Meteorol. 280, 107781 https://doi.org/10.1016/j.agrformet.2019.107781.

Zhang, B.B., Xu, Q., Gao, D.Q., Wang, T., Sui, M.Z., Huang, J., Gu, B.H., Liu, F.T., Jiang, J., 2021. Soil capacity of intercepting different rainfalls across subtropical plantation: Distinct effects of plant and soil properties. Sci. Total Environ. 784, 147120 https://doi.org/10.1016/j.scitotenv.2021.147120.

Zhang, Y.F., Yuan, C., Chen, N., Levia, D.F., 2023c. Rainfall partitioning by vegetation in China: A quantitative synthesis. J. Hydrol. 617, 128946 https://doi.org/10.1016/j.jhydrol.2022.128946.

Zhao, W.Y., Ji, X.B., Jin, B.W., Du, Z.Y., Zhang, J.L., Jiao, D.D., Zhao, L.W., 2023. Experimental partitioning of rainfall into throughfall, stemflow and interception loss by *Haloxylon ammodendron*, a dominant sand-stabilizing shrub in northwestern China. Sci. Total Environ. 858, 159928 https://doi.org/10.1016/j.scitotenv.2022.159928.

Zhao, G., Mu, X., Wen, Z., Wang, F., Gao, P., 2013. Soil erosion, conservation, and eco-environment changes in the Loess Plateau of China. Land Degrad Dev. 24 (5), 499–510. https://doi.org/10.1002/ldr.2246.

Zhu, X., He, Z.B., Du, J., Chen, L.G., Lin, P.F., Tian, Q.Y., 2021. Spatial heterogeneity of throughfall and its contributions to the variability in near-surface soil water-content in semiarid mountains of China. For. Ecol. Manage. 488 (6), 119008 https://doi.org/10.1016/j.foreco.2021.119008.

Zong, H., Chen, Y.Y., Liu, L., Zhang, L., Chen, X.H., 2021. Influence of rainfall factors and tree structure on rainfall partitioning for typical trees in Linpan settlements, the typical agroforestry ecosystem of the Chengdu Plain. J. Hydrol: Reg. Stud. 36, 100874 https://doi.org/10.1016/j.ejrh.2021.100874.